

N^* Experiments and what they tell us about Strong QCD Physics

V. D. Burkert

December 25, 2019

Abstract I give an overview on experimental studies of the spectrum and the structure of the excited states of the nucleon and what we can learn about their internal structure. One focus is on the efforts to obtain a more complete picture of the light-quark baryon excitation spectrum employing electromagnetic beams that will allow us to draw some conclusions on the symmetries underlying the spectrum. For the higher mass excitations, the full employment of coupled channel approaches is essential when searching for new excited states in the large amounts of data already accumulated in different channels involving a variety of polarization observables. The other focus is on the study of transition form factors and helicity amplitudes and their dependences on Q^2 , especially on some of the more prominent resonances, especially $\Delta(1232)_{\frac{3}{2}^+}$, $N(1440)_{\frac{1}{2}^+}$, and negative parity states $N(1535)_{\frac{1}{2}^-}$, and $N(1675)_{\frac{5}{2}^-}$. These were obtained in pion and eta electroproduction experiments off proton targets and have already led to further insights in the active degrees-of-freedom as a function of the distance scale involved.

Keywords light-quark baryon excitation, electroexcitation of nucleon resonances, quark core, meson-baryon contributions

PACS 12.39.Ki, 13.40.Gp, 13.40.Hq, 14.20.Gk

V.D. Burkert
Thomas Jefferson National Accelerator Facility
Newport News, Virginia 23606, USA
E-mail: burkert@jlab.org

1 Excited baryon states in the history of the Universe

For this talk the organizers asked me to address what we learn about strong QCD (sQCD), i.e. QCD in the domain where perturbative methods fail in describing nucleon resonances transitions. Talking about a similar topic from the theory perspective, Nathan Isgur said this in the concluding talk at N^*2000 : "*I am convinced that completing this chapter in the history of science will be one of the most interesting and fruitful areas of physics for at least the next thirty years.*" We are now 19 years into this 30 years prediction, and the physics of N^* 's continues to go strong, while many related issues remain to be explored.

As we are trying to make progress in the complex world of physical sciences, we should not lose sight of what physics is all about: understanding the origin and the history of our universe, and the laws underlying the observations. In this meeting we also address how excited states of the nucleon fit in to our understanding of the forces and the dynamics of matter in the history of the universe. On the internet we find beautiful representations of the phases through which the universe evolved from the Big Bang (BB) to our times as shown in Fig. 1. There are some marked events that have been of particular significance during the early phases of the its history, such as the quark-gluon plasma of non-interacting colored quarks and gluons, and the forming of protons and neutrons. During this transition dramatic events occur - chiral symmetry is broken, quarks acquire mass dynamically, baryon resonances occur abundantly, and colored quarks and gluons are confined. This crossover process is governed by the excited hadrons, this is schematically shown in the generic QCD phase diagram in Fig. 1. In this process strong

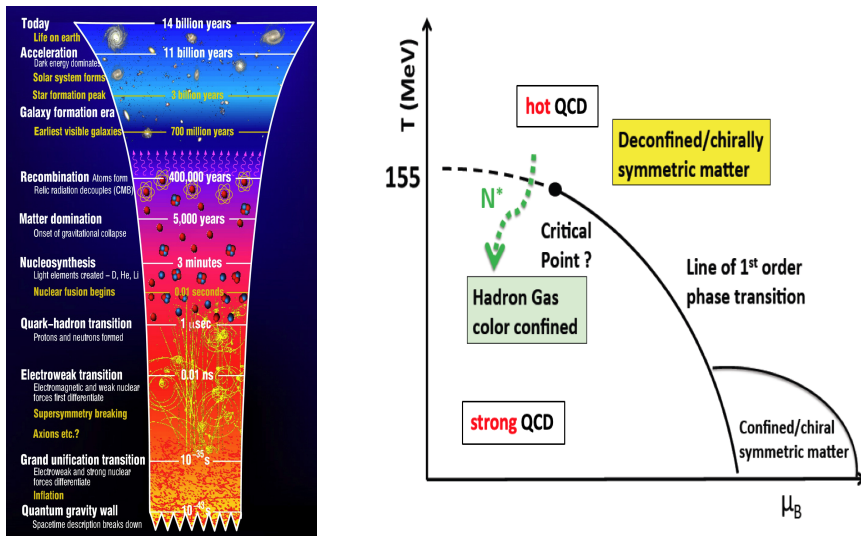


Fig. 1 Left panel: The evolution of the Universe. The line denoted as *Quark-hadron transition*, is where protons and neutrons are formed. Existing electron accelerators as CEBAF, ELSA, and MAMI, and colliders as BES III have sufficient energy reach to access this region and study processes in isolation that occurred during this transition in the microsecond old universe and resulted in the freeze out of baryons. Right panel: A generic phase diagram for the transition from the de-confined quark-gluon state to the confined hadron state.

QCD (sQCD) is born as the process describing the interaction of colored quarks and gluons. These are the phenomena that we are exploring with electron and hadron accelerators - the full discovery of the baryon (and meson) spectrum, the role of chiral symmetry breaking and the generation of dynamical quark mass in confinement. While we can not recreate the exact condition in the laboratory, with existing accelerators we can explore these processes in isolation. With electron machines and high energy photon beams in the few GeV energy range we search for undiscovered excitations of nucleons and other baryons.

As the Universe expands and cools down the coupling of quarks to the gluon field becomes stronger and quarks become more massive and form excited states in abundance. This eventually gives way to the forming stable nucleons. In the heavy-quark sector It has been demonstrated [1,2] that the entire complement of excited states as predicted in the quark model [3] is needed to be included in these calculation to explain what is observed in "hot QCD" lattice calculations. Including only resonances from the Review of Particle Physics (RPP) is insufficient to explain the computations within hot QCD. Similar projections have been made in the light-quark sector that we will discuss in the second part of this report. The close relationship of the baryon resonance spectrum and the evolution of the early universe makes the experimental search for the "missing resonances" an even more compelling experimental program.

2 Search for missing baryon states

Vigorous spectroscopy programs are currently underway at various particle accelerators in the quest for undiscovered excited mesons and baryons. Experiments at electron machines such as CEBAF at JLAB in the US, ELSA at Bonn University in Germany, and MAMI at the Johannes Gutenberg University at Mainz in Germany, focus on the s-channel excitation of protons and neutrons to N^* and Δ^* states.

The excited states of the nucleon have been studied experimentally since the 1950's [4]. They contributed to the discovery of the quark model in 1964 by Gell-Mann and Zweig [5,6], and were critical for the discovery of "color" degrees of freedom as first introduced by Greenberg [7]. The 3-quark quark structure of baryons resulted in the prediction of a wealth of excited states with underlying spin-flavor and orbital symmetry of $SU(6) \otimes O(3)$. The predictions led to a broad experimental effort to search for these states. Of the many states predicted in the quark model, only a fraction have been observed, even today. Searches for the "missing" states and detailed studies of the resonance structure are now mostly carried out using electromagnetic probes and have been a major focus of hadron physics for the past two decades [8]. A broad experimental effort has been underway for the past two decades, with measurements of exclusive meson photoproduction and electroproduction reactions, including many polarization observables. Precision data and the development of multi-channel partial wave analysis procedures have

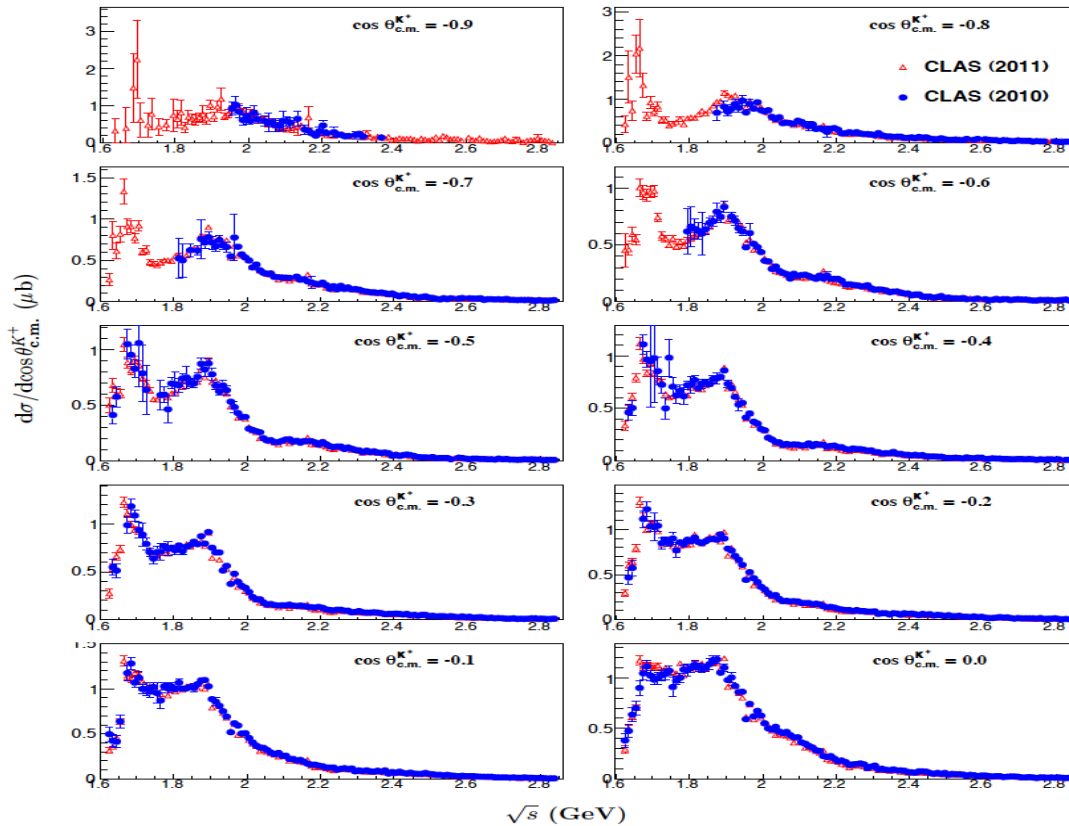


Fig. 2 Invariant mass dependence of the $\gamma p \rightarrow K^+ \Lambda$ differential cross section in the backward polar angle range. There are 3 structures visible that may indicate resonance excitations, at 1.7, 1.9, and 2.2 GeV. The blue full circles are based on the topology $K^+ p \pi^-$, the red open triangles are based on topology $K^+ p$ or $K^+ \pi^-$, which extended coverage towards lower W at backward angles and allows better access to the resonant structure near threshold.

resulted in the discovery of a series of excited states of the nucleon in the mass range of 1.9 to 2.2 GeV, others have been upgraded in their status of likelihood of existence as entered in the bi-annual Reviews of Particle Physics [9,10,11,12]. We will discuss some of these states in the following sections.

Accounting for the complete excitation spectrum of the nucleon (protons and neutrons) and understanding the effective degrees of freedom is perhaps the most important and certainly the most challenging task of hadron physics. The experimental N* program currently focusses on the search for new excited states in the mass range above 2 GeV using energy-tagged photon beams in the few GeV range, and the study of the internal structure of prominent resonances in meson electroproduction.

A quantitative description of baryon spectroscopy and the structure of excited nucleons must eventually

involve solving QCD for a complex strongly interacting multi-particle system. Recent advances in Lattice QCD led to predictions of the nucleon spectrum in QCD with dynamical quarks [13], albeit with still large pion masses of 396 MeV. Lattice prediction can therefore only be taken as indicative of the quantum numbers of excited states and not of the masses of specific states. In parallel, the development of dynamical coupled channel models is being pursued with new vigor. The EBAC group at JLab as well as others have shown [14] that dynamical effects can result in significant mass shifts of the excited states. As a particularly striking result, a very large shift was found for the Roper resonance pole mass to 1365 MeV downward from its bare mass of 1736 MeV. This result has clarified the longstanding puzzle of the incorrect mass ordering of $N(1440)\frac{1}{2}^+$ and $N(1535)\frac{1}{2}^-$ resonances in the constituent quark model. Developments on the phenomenological side go hand in

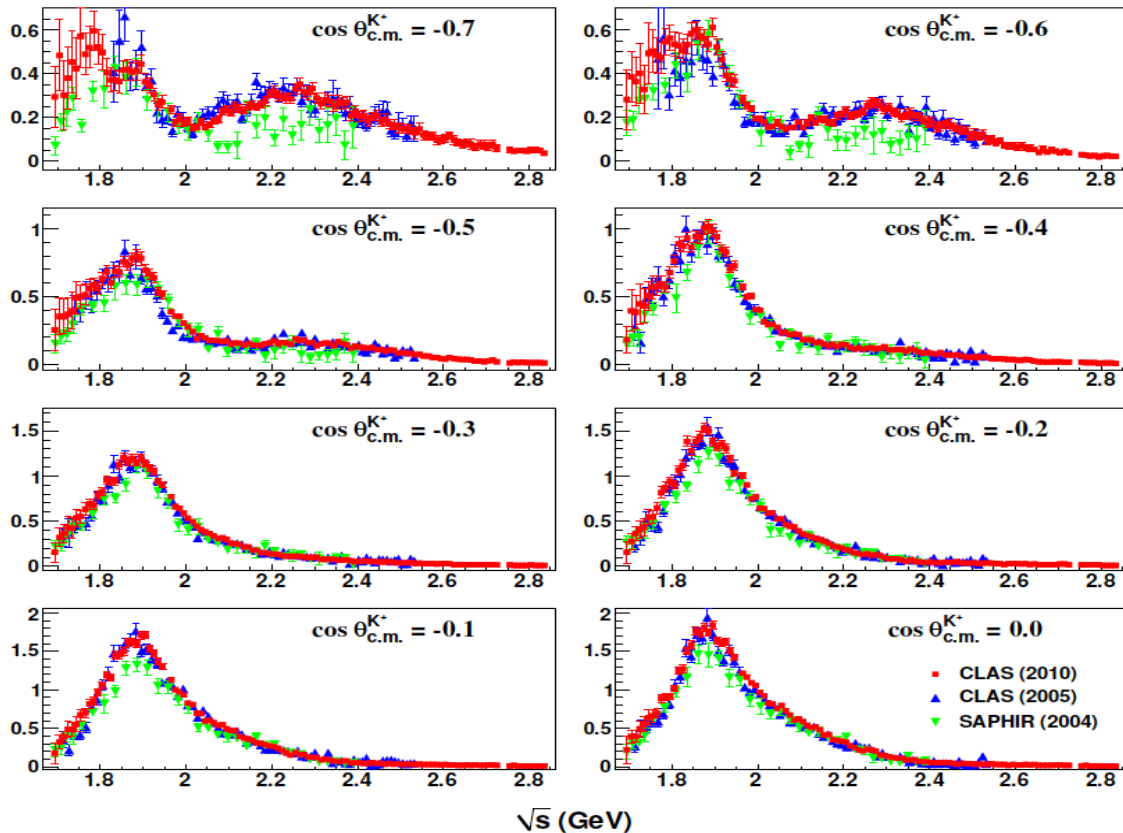


Fig. 3 Invariant mass dependence of the $\gamma p \rightarrow K^+ \Sigma^0$ differential cross section in the backward polar angle range.

hand with a world-wide experimental effort to produce high precision data in many different channel as a basis for a determination of the light-quark baryon resonance spectrum. On the example of experimental results from CLAS, the strong impact of precise meson photoproduction data is discussed. Several reviews have recently been published on this and related subjects [15,16,17, 18,19] where many details can be found.

3 Establishing the N^* Spectrum

The complex structure of the light-quark (u & d quarks) baryon excitation spectrum complicates the experimental search for individual states. As a result of the strong interaction, resonances are wide, often 200 MeV to 300 MeV, and are difficult to uniquely identify when only differential cross sections are measured. Most of the excited nucleon states listed in the Review of Particle Physics (RPP) prior to 2012 have been observed in elastic pion scattering $\pi N \rightarrow \pi N$. However there are

important limitations in the sensitivity to the higher mass nucleon states that may have very small $\Gamma_{\pi N}$ decay widths, and the extraction of resonance contributions then becomes exceedingly difficult in this channel.

Estimates for alternative decay channels have been made in quark model calculations[20] for various channels. This has led to a major experimental effort at Jefferson Lab, ELSA, GRAAL, and MAMI to chart differential cross sections and polarization observables for a variety of meson photoproduction channels. At JLab with CLAS, many different final states have been measured with high precision on the proton [21,22,23,24, 25,26,27,28,29,30,31,32,33,34,35,36,37], many of them are now employed in single- and in multi-channel analyses [38]. Recently, the first measurements of open strangeness processes on neutron targets have been published [39, 40].

State $N((\text{mass})J^P)$	PDG 2010	PDG 2018
$N(1710)1/2^+$	***	****
$N(1880)1/2^+$		***
$N(2100)1/2^+$	*	***
$N(1895)1/2^-$		****
$N(1900)3/2^+$	**	****
$N(1875)3/2^-$		***
$N(2120)3/2^-$		***
$N(2060)5/2^-$		***
$\Delta(1600)3/2^+$	***	****
$\Delta(1900)1/2^-$	**	***
$\Delta(2200)7/2^-$	*	***

Fig. 4 Evidence for 11 N and Δ states in RPP 2010 compared with RPP 2018 [12].

3.1 New states from open strangeness photoproduction

Here one focus has been on measurements of $\gamma p \rightarrow K^+ \Lambda$ and $\gamma p \rightarrow K^+ \Sigma$. Using a linearly polarized photon beam several polarization observables can be measured by analyzing the parity violating decay of the recoil $\Lambda \rightarrow p\pi^-$. It is well known that the energy-dependence of a partial-wave amplitude for one particular channel is influenced by other reaction channels due to unitarity constraints. To fully describe the energy-dependence of a production amplitude other reaction channels must be included in a coupled-channel approach. Such analyses have been developed by the Bonn-Gatchina group[41], at JLab[42], at Jülich[43] and other groups. More recent measurements of single and double polarization data in the same channel [33] are shown in Fig. 8.

The data sets with the highest impact on resonance amplitudes in the mass range above 1.7 GeV have been kaon-hyperon production using a spin-polarized photon beam and the polarization of the Λ or Σ^0 is also measured by analyzing the parity violating decay $\Lambda \rightarrow p\pi^-$. The high precision cross section and polarization data [29,30,32,35,36] provide nearly full polar angle coverage and span the $K^+ \Lambda$ invariant mass range from threshold to 2.9 GeV, hence covering the full nucleon resonance domain where new states could be discovered.

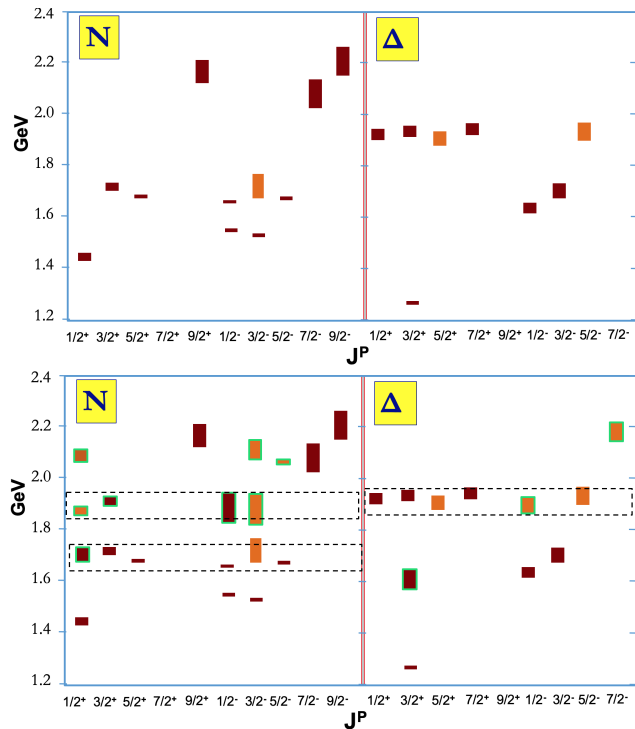


Fig. 5 Top panel: Nucleon and Δ resonance spectrum below 2.2 GeV in RPP 2010 [9]. Bottom panel: Nucleon and Δ resonance spectrum below 2.2 GeV in RPP 2018 [12]. The green frames highlight the new states and states with improved start ratings compared to 2010. The light brown color indicate 3* states, the dark color indicates 4* states. The dashed frames indicate apparent mass degeneracy of states with masses near 1.7 GeV and 1.9 GeV and different spin and parity. The Bonn-Gatchina analysis includes all the $K^+ \Lambda$ and $K^+ \Sigma^0$ cross section and polarization data, as well as pion photoproduction data.

The backward angle $K^+ \Lambda$ data in Fig.2 show clear resonance-like structures at 1.7 GeV and 1.9 GeV that are particularly prominent and well-separated from other structures at backward angles, while at more forward angles (not shown) t-channel processes become prominent and dominate the cross section. The broad enhancement at 2.2 GeV may also indicate resonant behavior although it is less visible at more central angles with larger background contributions. The $K^+ \Sigma$ channel also indicates significant resonant behavior as seen in Fig. 3. The peak structure at 1.9 GeV is present at all angles with a maximum strength near 90 degrees, consistent with the behavior of a $J^P = \frac{3}{2}^+$ p-wave. Other structures near 2.2 to 2.3 GeV are also visible. Still, only a full partial wave analysis can determine the underlying resonances, their masses and spin-parity. The task is somewhat easier for the $K \Lambda$ channel, as the iso-scalar nature of the Λ selects isospin- $\frac{1}{2}$ states to contribute to the $K \Lambda$ final state, while both isospin- $\frac{1}{2}$ and isospin- $\frac{3}{2}$ states can contribute to the $K \Sigma$ final state.

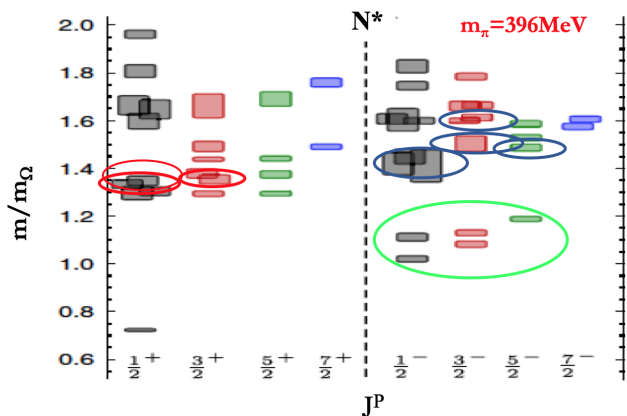


Fig. 6 Nucleon resonance spectrum below 2.2 GeV from LQCD [45]. The new discovered Nucleon states from RPP 2018 [12] are indicated by the red and blue ellipses with their spin-parity assignments. The observed masses deviate from the predicted ones as the lattice calculation used 396MeV pion mass, and no multi channel coupling is included. The green ellipses are well-known states that come out in the LQCD work with higher masses.

These cross section data together with the Λ and Σ recoil polarization and polarization transfer data to the Λ and Σ had strong impact on the discovery of several new nucleon states [44]. They also provided new evidence for several candidate states that had been observed previously but lacked confirmation as shown in Fig. 4. It is interesting to observe that four of the observed nucleon states have nearly degenerate masses near 1.9 GeV, as seen in Fig. 5. Similarly, the new Δ state appears to complete a mass degenerate multiplet near 1.9 GeV as well. There is no obvious mechanism for this apparent degeneracy. Nonetheless, all new states may be accommodated within the symmetric constituent quark model based on $SU(6) \otimes O(3)$ symmetry group as far as quantum numbers are concerned. As discussed in section 1 for the case of the Roper resonance $N(1440)\frac{1}{2}^+$, the masses of all pure quark model states need to be corrected for dynamical coupled channel effects to compare them with observed resonances. The same applies to the Lattice QCD predictions [45] for the nucleon and Delta spectrum.

Coming back to the evolution of the early universe, we may check what is the expected effect of these newly discovered states on the evolution of the universe near the cross over temperature $T_c \approx 155$ MeV? Figure 7 shows the ratio of the baryon chemical potential of strangeness carrying baryons over all baryons versus temperature near the crossover temperature between de-confined and confined and conditions. The graph clearly shows the significant impact of the recently included new baryons by the PDG in the 2016 edition of the RPP in comparison to the 2012 edition. Fur-

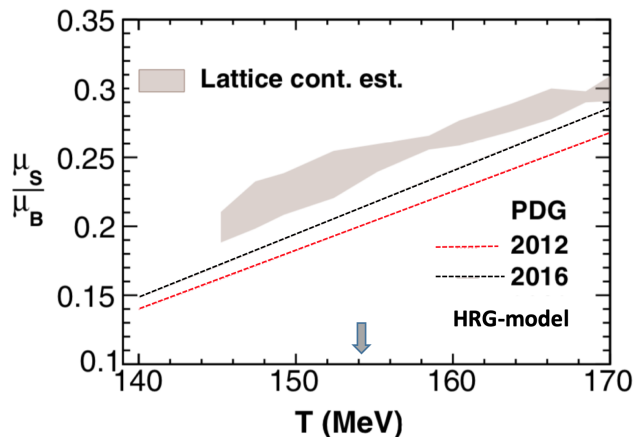


Fig. 7 The ratio of baryon chemical potential of strangeness versus all baryons for the RPP 2014 and RPP 2016. The hashed grey area show the LQCD calculation in "hot QCD". The straight lines are calculations within a hadron gas model. The 2016 line, which includes more N/Δ baryon states are included. Note that only 3^* and 4^* states are included. If the newly discovered states in RPP 2018 (seven states that are now at 3^* or 4^* status) were included this line would be moving even closer to the LQCD area.

thermore, adding new states found since 2016 and now included in the 2018 edition of RPP will bring the HRG model closer to the Lattice QCD calculation [46], demonstrating the strong impact excited nucleon states have in the transition from the phase of free colored quarks and gluons to quarks and gluons confined in protons and neutrons.¹

3.2 Vector meson photoproduction

Double-polarization measurements of single pion photoproduction data [34] have contributed significantly to the discovery of the high-mass $\Delta(2200)7/2^-$ state [47], although the state couples just at the 3.5% level to $N\pi$. Nevertheless in the mass range above 2.0 GeV resonances tend to decouple from simple final states like $N\pi$, $N\eta$, and $K\Lambda$, the search for undiscovered high-mass states requires to consider more complex final states with multi-mesons $N\pi\pi$ or vector mesons, such as $N\omega$, $N\phi$, and $K^*\Sigma$. The study of such final states adds significant complexity as many more amplitudes can contribute to these photoproduction processes compared to single pseudo-scalar meson production. As is the case for $N\eta$ production, the $N\omega$ channel is selective to isospin $\frac{1}{2}$ nucleon states only. The CLAS collaboration has collected a tremendous amount of data in the $p\omega$ channel [27,28], including single and double polar-

¹ Increasing the number of excited baryons will lower μ_B at a given temperature, and hence increase the ratio of $\frac{\mu_S}{\mu_B}$.

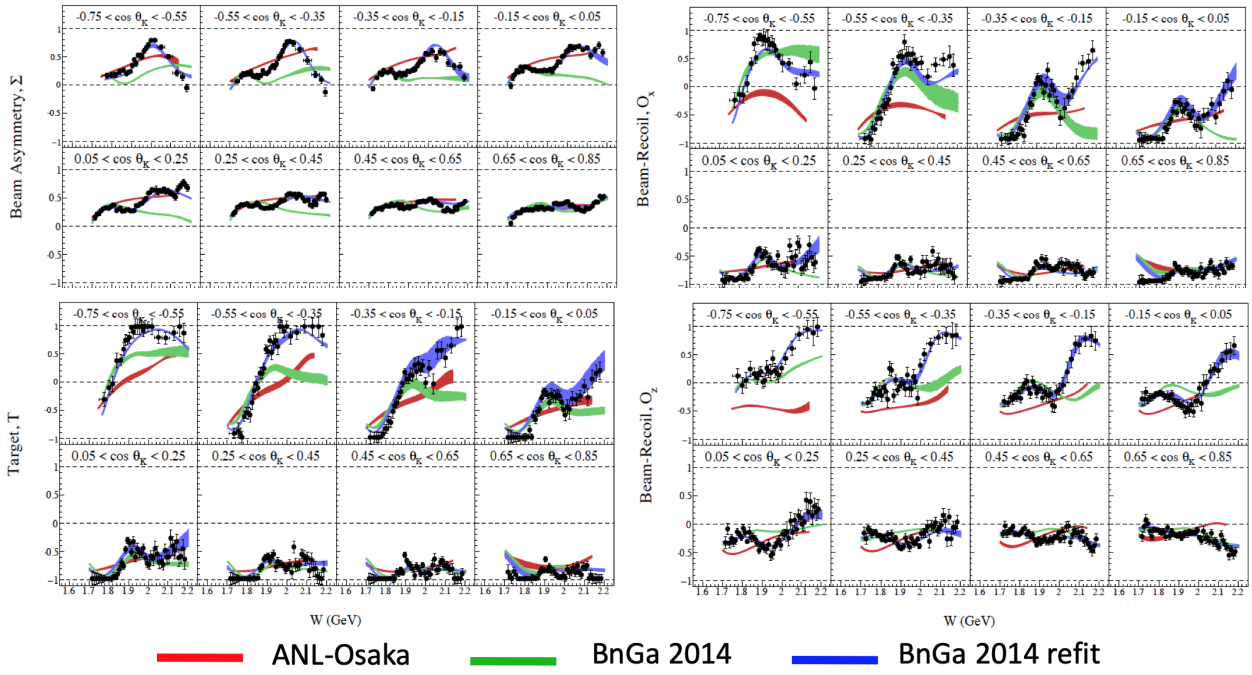


Fig. 8 Beam and Target polarization asymmetries (left panel), and beam-recoil polarization asymmetries (right panel) measured by the CLAS collaboration in the $\gamma p \rightarrow K^+ \Lambda$ channel. The projections from earlier analyses, shown in the red and green bands, show large discrepancies with the data in the higher W range. A refit by the BnGa group (blue band) shows that the discrepancies do not require new excited states but could be accommodated by just adjusting some parameters.

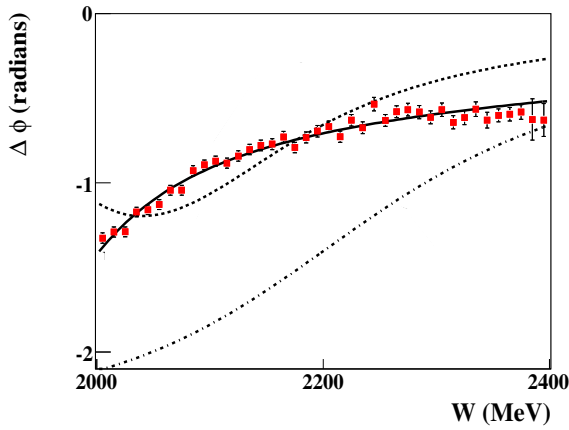


Fig. 9 Phase motion of the partial wave fit to the $\gamma p \rightarrow p \phi$ differential cross section and spin density matrix elements. 3 resonant states, the subthreshold resonance $N(1680)_{\frac{1}{2}^+}$, $N(2190)_{\frac{7}{2}^-}$, and the missing $N(2000)_{\frac{5}{2}^+}$ are needed to fit the data (solid line). Fits without $N(2000)_{\frac{5}{2}^+}$ (dashed-dotted line), or without $N(1680)_{\frac{1}{2}^+}$ (dashed line) cannot reproduce the data.

polarization measurements [48, 49, 50, 51, 52]. The CLAS collaboration performed a single channel event-based analysis, whose results are shown in Fig. 9, and provided further evidence for the $N(2000)_{\frac{5}{2}^+}$. Also a large amount

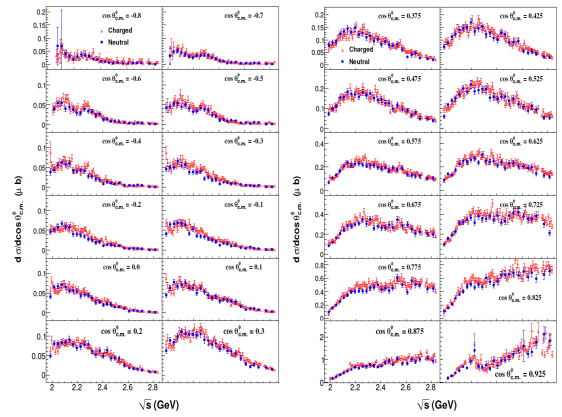


Fig. 10 Differential cross sections in a nearly full angular range for $\gamma p \rightarrow p \phi$ production.

of $p \phi$ [53, 54] final states on differential cross sections and spin-density matrix elements have been published, although they have not systematically included in the more complex multi-channel analyses. Photoproduction of ϕ mesons is also considered a potential source of new excited nucleon states in the mass range above 2 GeV. Differential cross sections and spin-density matrix elements have been measured for $\gamma p \rightarrow p \phi$ in a mass range

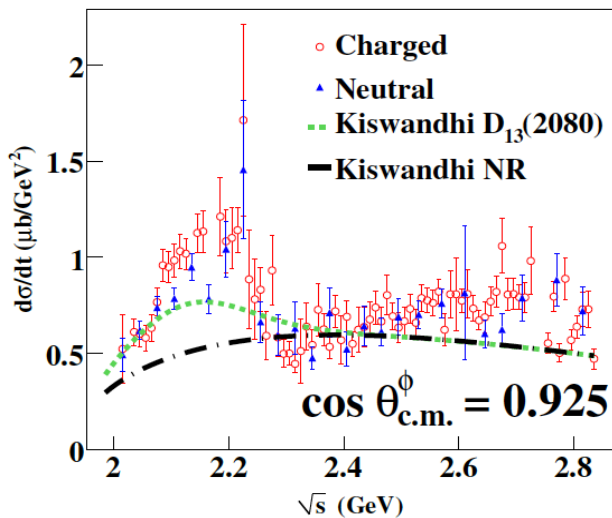


Fig. 11 Differential cross sections of $\gamma p \rightarrow p\phi$ production for the most forward angle bin. The two curves refer to fits without (dashed) and with (dotted) a known resonance at 2.08 GeV included.

up to nearly 3 GeV. In Fig. 10 structures are seen near 2.2 GeV in the forward most angle bins and at very backward angles for both decay channels $\phi \rightarrow K^+K^-$ and $\phi \rightarrow K_1^0 K_s^0$, and with the exception of the smallest forward angle bin the structures are more prominent at backward angles. Only a multi-channel partial wave analysis will be able to pull out any significant resonance strength. Fig. 11 shows the differential cross section $d\sigma/dt$ of the most forward angle bin. A broad structure at 2.2 GeV is present, but does not show the typical Breit-Wigner behavior of a single resonance. It also does not fit the data in a larger angle range, which indicates that contributions other than genuine resonances may be significant. The forward and backward angle structures may also hint at the presence of dynamical effects possibly due to molecular contributions such as diquark-anti-triquark contributions [55], the strangeness equivalent to the recently observed hidden charm P_c^+ states. Another process that has promise in the search for new excited baryon states, including those with isospin- $\frac{3}{2}$ is $\gamma p \rightarrow K^*\Sigma$ [56]. In distinction to the vector mesons discussed above, diffractive processes do not play a role in this channel, which then may allow better direct access to s-channel resonance production.

4 Structure of excited nucleons

Meson photoproduction has become an essential tool in the search for new excited baryons. The exploration of

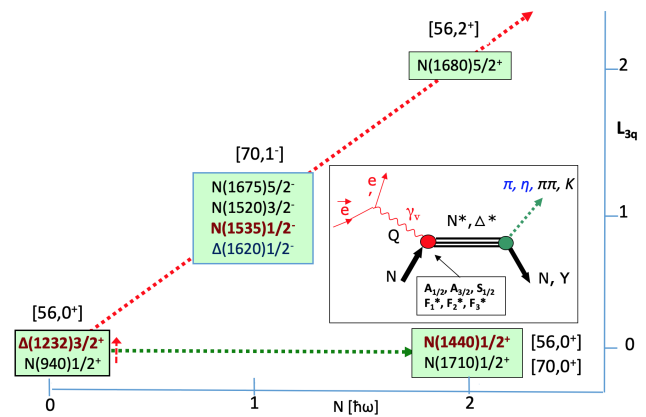


Fig. 12 Schematics of $SU(6) \otimes O(3)$ supermultiplets with some of the excited states that have been explored in $ep \rightarrow e'\pi^+n$, $ep \rightarrow e'p\pi^0$, $ep \rightarrow e'p\eta$, and $ep \rightarrow e'p\pi^+\pi^-$ electroproduction experiments. The inset shows the helicity amplitudes and electromagnetic multipoles often used to describe the data. Only the states highlighted in red are discussed here.

the internal structure of excited states and the effective degrees of freedom contributing to s-channel resonance excitation requires the use of electron beams, where the virtuality (Q^2) of the exchanged photon can be varied to probe the spatial structure. Electroproduction of final states with pseudoscalar mesons (e.g. $N\pi$, $p\eta$, $K\Lambda$) have been employed with CLAS, leading to new insights into the scale dependence of effective degrees of freedom, e.g. meson-baryon, constituent quark, and dressed quark contributions. Several excited states, shown in Fig. 12 assigned to their primary $SU(6) \otimes O(3)$ supermultiplets have been studied. The $N\Delta(1232)\frac{3}{2}^+$ transition is now well measured in a large range of Q^2 [57, 58, 59]. Results on the magnetic transition form factor G_{Mn} and on the quadrupole transition ratios are shown in Fig. 13 and Fig. 14. Two of the prominent higher mass states, the Roper resonance $N(1440)\frac{1}{2}^+$ and $N(1535)\frac{1}{2}^-$ are shown in Fig. 15 and in Fig. 17, respectively, as representative examples [60, 61, 63] of a wide program at JLab [64, 65, 66, 67, 68, 69, 70, 71, 72]. For these three states advanced relativistic quark model calculations [73] and QCD calculations from DSE [74] and Light Cone sum rule [75] are available, for the first time employing QCD-based modeling of the excitation of the quark core.

There is agreement with the data at $Q^2 > 1.5 \text{ GeV}^2$ for the latter two states, while the meson-baryon contributions for the $\Delta(1232)$ are more extended, and agreement with the quark based calculations is reached at $Q^2 > 4 \text{ GeV}^2$. The calculations deviate significantly from the data at lower Q^2 , which indicates significant non quark core effects. For the Roper resonance such

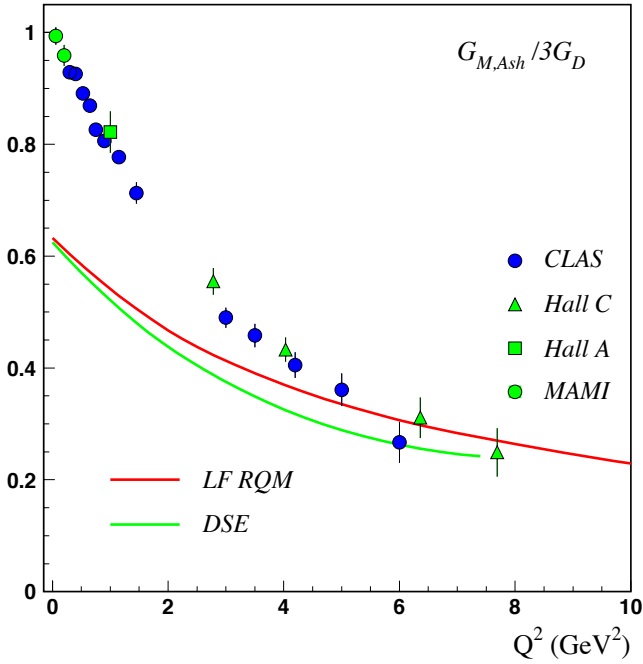


Fig. 13 (Color online) The magnetic $N\Delta$ transition form factor normalized to the dipole form factor compared with the LF RQM with running quark mass, and with DSE/QCD. Both are close to the data at high Q^2 . At $Q^2 < 3\text{GeV}^2$ meson-baryon contributions are significant.

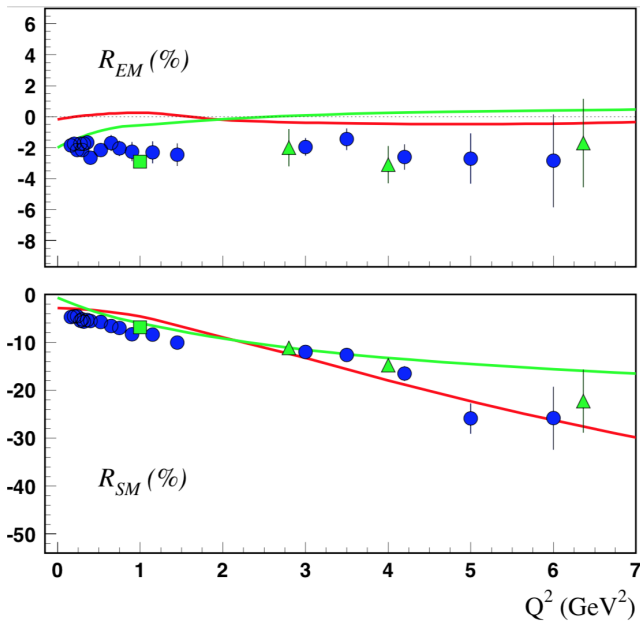


Fig. 14 (Color online) The ratios R_{EM} and R_{SM} for the $N\Delta(1232)$ transition. The solid red curves are the LF RQM predictions, the green curves are from the DSE approach. References to data as in Fig. 13.

contributions have been described successfully in dynamical meson-baryon models [76] and in effective field theory [77]. Calculations on the Lattice for the N-Roper

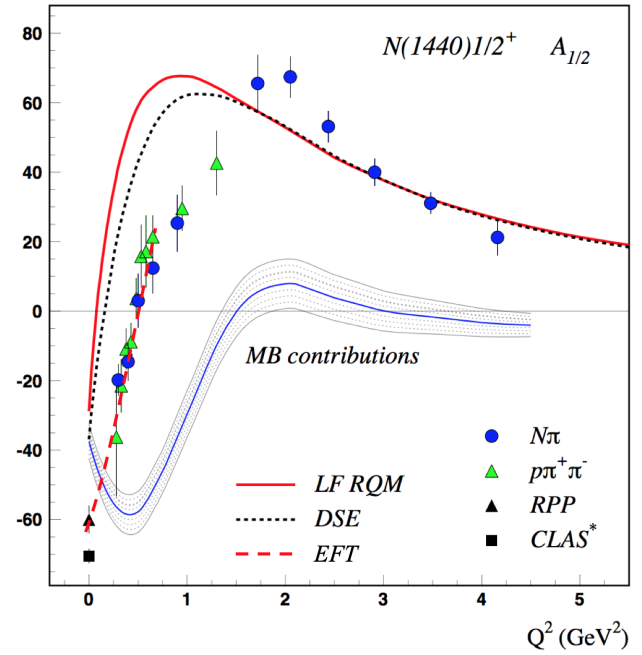


Fig. 15 The transverse helicity amplitudes $A_{1/2}$ for the Roper resonance $N(1440)\frac{1}{2}^+$. Data are from CLAS compared to LF RQM with running quark masses (solid line), and with projections from the DSE/QCD approach (dotted line). The shaded band indicates non-3-quark contributions inferred from the difference of the LF RQM curve and the CLAS data. The red dashed line is the EFT calculation that describes the data at small Q^2 .

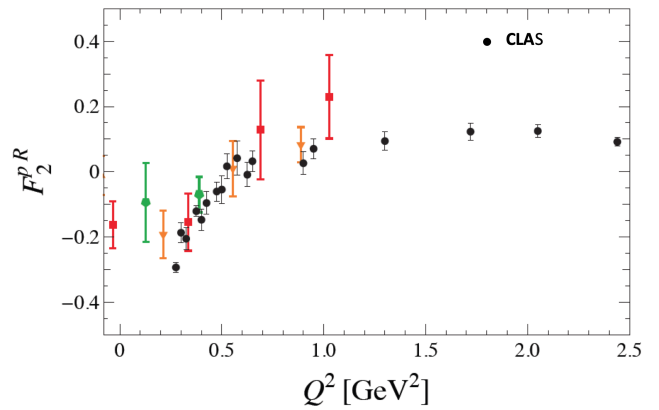


Fig. 16 The $pN^+(1440)\frac{1}{2}^+$ transition amplitude $F_2(Q^2)$ from LQCD [62] compared to CLAS results.

transition amplitudes have been carried out with dynamical quarks [62]. The results agree with the data in the range $Q^2 < 1.0\text{GeV}^2$, where data and calculations overlap Fig. 16.

Knowledge of the helicity amplitudes in a large Q^2 allows for the determination of the transition charge densities on the light cone in transverse impact parameter space (b_x, b_y) [78]. Figure 18 shows the comparison

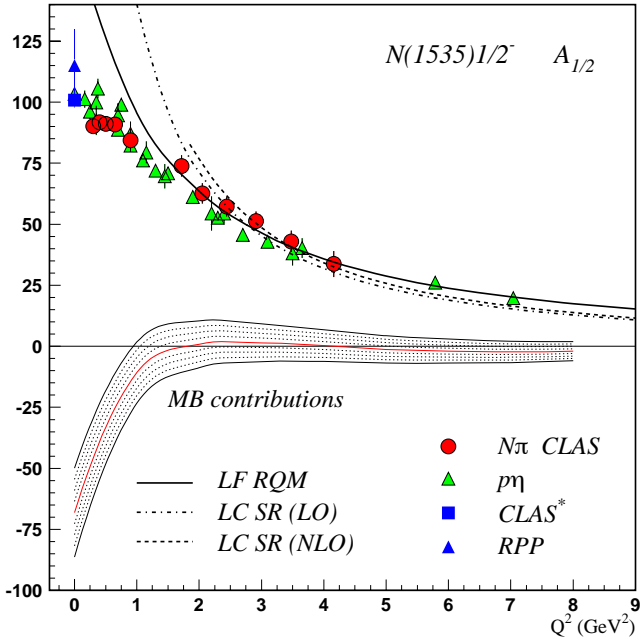


Fig. 17 The transverse amplitude $A_{1/2}$ for the $N(1535)\frac{1}{2}^-$ resonance compared to LF RQM calculations (solid line) and QCD computation within the LC Sum Rule approach.

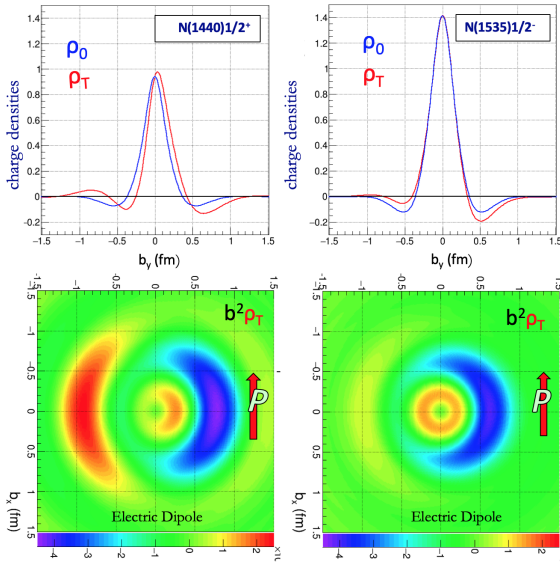


Fig. 18 Left panels: $N(1440)$, top: projection of charge densities on b_y , bottom: transition charge densities when the proton is spin polarized along b_x . Right panels: same for $N(1535)$. Note that the densities are scaled with b^2 to emphasize the outer wings. Color code: negative charge is blue, positive charge is red. Note that all scales are the same.

of $N(1440)\frac{1}{2}^+$ and $N(1535)\frac{1}{2}^-$. There are clear differences in the charge transition densities between the two states. The Roper state has a softer positive core and a wider negative outer cloud than $N(1535)$ and develops a larger shift in b_y when the proton is polarized along the b_x axis. New electroproduction data on the Roper

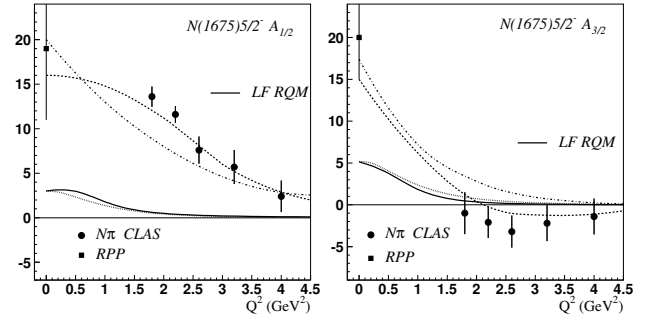


Fig. 19 Helicity amplitude $A_{1/2}$ (left) and $A_{3/2}$ (right) for $N^+(1675)5/2^-$ off proton target.

and several higher mass states have been obtained in the 2-pion channel, specifically in $ep \rightarrow e'p\pi^+\pi^-$ [65].

4.1 The $N(1675)5/2^-$ state - revealing the meson-baryon contributions

In previous discussions we have assumed that meson-baryon degrees of freedom provide significant strength to the resonance excitation in the low Q^2 domain where quark based approaches LF RQM, DSE/QCD, and LCSR calculations fail to reproduce the transition amplitudes quantitatively. Our conclusion rests, in part, with this assumption. But, how can we be certain of the validity of this assumption?

The $N(1675)5/2^-$ resonance allows testing this assumption, quantitatively. Figure 19 shows our current knowledge of the transverse helicity amplitudes $A_{1/2}(Q^2)$ and $A_{3/2}(Q^2)$, for proton target compared to RQM [79] and hypercentral CQM [80] calculations. The specific quark transition for a $J^P = 5/2^-$ state belonging to the $SU(6) \otimes O(3) = [70, 1^-]$ supermultiplet configuration, in non-relativistic approximation prohibits the transition from the proton in a single quark transition. This suppression, known as the Moorhouse selection rule [81], is valid for the transverse transition amplitudes $A_{1/2}$ and $A_{3/2}$ at all Q^2 . It should be noted that this selection rule does apply to the transition from protons but not from neutrons. Modern quark models, that go beyond single quark transitions, confirm quantitatively the suppression resulting in very small transition amplitudes from protons but large ones from neutrons. The measured helicity amplitudes off the protons are almost exclusively due to meson-baryon contributions as the dynamical coupled channel (DCC) calculation indicates (dashed line). The close correlation of the DCC calculation and the measured data for the case when quark contributions are nearly absent, supports the phenomenological description of the helicity amplitudes in terms of a 3-quark core that dominate

at high Q^2 and meson-baryon contributions that can make important contributions at lower Q^2 .

5 Conclusions and Outlook

Over the past five years eight baryon states in the mass range from 1.85 to 2.15 GeV have been either discovered or evidence for the existence of states has been significantly strengthened. To a large degree this is the result of adding very precise photoproduction data in open strangeness channels to the data base that is included in multi-channel partial wave analyses, especially the Bonn-Gatchina PWA. The possibility to measure polarization observables in these processes has been critical. In the mass range above 2 GeV more complex processes such as vector mesons or $\Delta\pi$ may have sensitivity to states with higher masses but require more complex analyses techniques to be brought to bear. Precision data in such channels have been available for a few years but remain to be fully incorporated in multi-channel partial wave analyses processes. The light-quark baryon spectrum is likely also populated with hybrid excitations [13] where the gluonic admixtures to the wave function are dominating the excitation. These states appear with the same quantum numbers as ordinary quark excitations, and can only be isolated from ordinary states due to the Q^2 dependence of their helicity amplitudes [82], which is expected to be quite different from ordinary quark excitations. This requires new electroproduction data especially at low Q^2 [83] with different final states and at masses above 2 GeV.

Despite the very significant progress made in recent years to further establish the light-quark baryon spectrum and explore the internal structure of excited states, much remains to be done. A vast amount of precision data already collected needs to be included in the multi-channel analysis frameworks, and polarization data are still to be analyzed.

There are approved proposals to study resonance excitations at much higher Q^2 and with higher precision at Jefferson Lab with CLAS12 [84,85], which may reveal the transition to the bare quark core contributions at short distances.

A new avenue of experimental research has recently been opened up with the data-based extraction of the first mechanical property of the proton - its internal pressure distribution [86]. Mechanical properties of resonance transitions have recently been explored for the $N(1535)3/2^- \rightarrow N(938)$ gravitational transition form factors calculations [87]. In order to access these new gravitational form factors experimentally, the nucleon to resonance transition GPDs have to be studied. The framework for studying the $N \rightarrow N(1535)$ transition

GPDs, which would enable experimental access to these mechanical properties, still remains to be developed.

I like to thank Inna Aznauryan and Viktor Mokeev for numerous discussions on the subjects discussed in this presentation.

6 Acknowledgment

This work was supported by the US Department of Energy under contract No. DE-AC05-06OR23177. This work was supported by the U.S. Department of Energy, Office of Science, Office of Nuclear Physics, under Contract No. DE-AC05-06OR23177.

References

1. A. Bazavov *et al.*, Phys. Rev. Lett. **113**, 072001 (2014) doi:10.1103/PhysRevLett.113.072001 [arXiv:1404.6511 [hep-lat]].
2. A. Bazavov *et al.*, Phys. Lett. B **737**, 210 (2014) doi:10.1016/j.physletb.2014.08.034 [arXiv:1404.4043 [hep-lat]].
3. S. Capstick and N. Isgur, Phys. Rev. D **34**, 2809 (1986) [AIP Conf. Proc. **132**, 267 (1985)]. doi:10.1103/PhysRevD.34.2809, 10.1063/1.35361
4. H. L. Anderson, E. Fermi, E. A. Long and D. E. Nagle (1952) Phys. Rev. **85**, 936 .
5. M. Gell-Mann, Phys. Lett. **8**, 214 (1964).
6. G. Zweig, CERN Reports, TH 401 and 412 (1964).
7. O. W. Greenberg, Phys. Rev. Lett. **13**, 598 (1964); arXiv:0803.0992 [physics.hist-ph].
8. V. D. Burkert and T. S. H. Lee Int. J. Mod. Phys. E **13**, 1035 (2004).
9. J. Beringer *et al.* [Particle Data Group], Phys. Rev. D **86**, 010001 (2012). doi:10.1103/PhysRevD.86.010001
10. K. A. Olive *et al.* [Particle Data Group], Chin. Phys. C **38**, 090001 (2014). doi:10.1088/1674-1137/38/9/090001
11. C. Patrignani *et al.* [Particle Data Group], Chin. Phys. C **40**, no. 10, 100001 (2016). doi:10.1088/1674-1137/40/10/100001
12. M. Tanabashi *et al.* [Particle Data Group], Phys. Rev. D **98**, no. 3, 030001 (2018). doi:10.1103/PhysRevD.98.030001
13. J. J. Dudek and R. G. Edwards, Phys. Rev. D **85**, 054016 (2012)
14. N. Suzuki *et al.*, Phys. Rev. Lett. **104**, 042302 (2010) [arXiv:0909.1356 [nucl-th]].
15. E. Klempt and J. M. Richard, Rev. Mod. Phys. **82**, 1095 (2010)
16. L. Tiator, D. Drechsel, S. S. Kamalov and M. Vanderhaeghen, Eur. Phys. J. ST **198**, 141 (2011).
17. I. G. Aznauryan and V. D. Burkert, Prog. Part. Nucl. Phys. **67**, 1 (2012)
18. I. G. Aznauryan *et al.*, Int. J. Mod. Phys. E **22**, 1330015 (2013)
19. V. Crede and W. Roberts, Rept. Prog. Phys. **76**, 076301 (2013)
20. S. Capstick and W. Roberts, Phys. Rev. D **49**, 4570 (1994)
21. M. Dugger *et al.*, Phys. Rev. Lett. **96**, 062001 (2006) [Phys. Rev. Lett. **96**, 169905 (2006)]

22. M. Dugger *et al.* [CLAS], Phys. Rev. C **79**, 065206 (2009) doi:10.1103/PhysRevC.79.065206
23. P. T. Mattione *et al.* [CLAS], Phys. Rev. C **96**, no. 3, 035204 (2017) doi:10.1103/PhysRevC.96.035204
24. I. Senderovich *et al.* [CLAS], Phys. Lett. B **755** (2016) 64 doi:10.1016/j.physletb.2016.01.044
25. M. Williams *et al.* [CLAS Collaboration], Phys. Rev. C **80**, 045213 (2009)
26. P. Collins *et al.* [CLAS], Phys. Lett. B **771**, 213 (2017) doi:10.1016/j.physletb.2017.05.045
27. M. Williams *et al.* [CLAS], Phys. Rev. C **80**, 065209 (2009)
28. M. Williams *et al.* [CLAS], Phys. Rev. C **80**, 065208 (2009)
29. R. K. Bradford *et al.* [CLAS], Phys. Rev. C **75**, 035205 (2007)
30. R. Bradford *et al.* [CLAS], Phys. Rev. C **73**, 035202 (2006)
31. D. Ho *et al.* [CLAS], Phys. Rev. Lett. **118**, no. 24, 242002 (2017) doi:10.1103/PhysRevLett.118.242002
32. M. E. McCracken *et al.* [CLAS], Phys. Rev. C **81**, 025201 (2010)
33. C. A. Paterson *et al.* [CLAS], Phys. Rev. C **93**, no. 6, 065201 (2016) doi:10.1103/PhysRevC.93.065201
34. S. Strauch *et al.* [CLAS], Phys. Lett. B **750**, 53 (2015) doi:10.1016/j.physletb.2015.08.053
35. B. Dey *et al.* [CLAS], Phys. Rev. C **82**, 025202 (2010)
36. J. W. C. McNabb *et al.* [CLAS], Phys. Rev. C **69**, 042201 (2004)
37. E. Golovatch *et al.* [CLAS], Phys. Lett. B **788**, 371 (2019) doi:10.1016/j.physletb.2018.10.013
38. A. V. Anisovich *et al.*, Phys. Lett. B **772**, 247 (2017) doi:10.1016/j.physletb.2017.06.052
39. N. Compton *et al.* [CLAS], Phys. Rev. C **96**, no. 6, 065201 (2017) doi:10.1103/PhysRevC.96.065201
40. D. Ho *et al.* [CLAS], Phys. Rev. C **98**, no. 4, 045205 (2018) doi:10.1103/PhysRevC.98.045205
41. A. Anisovich, R. Beck, E. Klempt, V. Nikonov, A. Sarantsev and U. Thoma, Eur. Phys. J. A **48**, 15 (2012)
42. B. Julia-Diaz, T.-S. H. Lee, A. Matsuyama and T. Sato, Phys. Rev. C **76**, 065201 (2007)
43. D. Rönchen *et al.*, Eur. Phys. J. A **50**, no. 6, 101 (2014)
44. A. V. Anisovich *et al.*, Phys. Rev. Lett. **119**, no. 6, 062004 (2017) doi:10.1103/PhysRevLett.119.062004 [arXiv:1712.07549 [nucl-ex]].
45. R. G. Edwards, J. J. Dudek, D. G. Richards and S. J. Wallace, Phys. Rev. D **84**, 074508 (2011) doi:10.1103/PhysRevD.84.074508 [arXiv:1104.5152 [hep-ph]].
46. S. Chatterjee, D. Mishra, B. Mohanty and S. Samanta, Phys. Rev. C **96**, no. 5, 054907 (2017) doi:10.1103/PhysRevC.96.054907 [arXiv:1708.08152 [nucl-th]].
47. A. V. Anisovich *et al.*, Phys. Lett. B **766**, 357 (2017) doi:10.1016/j.physletb.2016.12.014
48. P. Collins *et al.* [CLAS], Phys. Lett. B **773**, 112 (2017) doi:10.1016/j.physletb.2017.08.015
49. Z. Akbar *et al.* [CLAS], Phys. Rev. C **96**, no. 6, 065209 (2017) doi:10.1103/PhysRevC.96.065209 [arXiv:1708.02608 [nucl-ex]].
50. P. Roy *et al.* [CLAS], Phys. Rev. C **97**, no. 5, 055202 (2018) doi:10.1103/PhysRevC.97.055202
51. P. Roy *et al.* [CLAS], Phys. Rev. Lett. **122**, no. 16, 162301 (2019) doi:10.1103/PhysRevLett.122.162301
52. A. V. Anisovich *et al.* [CLAS], Phys. Lett. B **771**, 142 (2017). doi:10.1016/j.physletb.2017.05.029
53. H. Seraydaryan *et al.* [CLAS Collaboration], Phys. Rev. C **89**, no. 5, 055206 (2014)
54. B. Dey *et al.* [CLAS Collaboration], Phys. Rev. C **89**, no. 5, 055208 (2014)
55. R. F. Lebed, Phys. Rev. D **92**, no. 11, 114030 (2015)
56. A. Sarantsev, talk at this workshop
57. K. Joo *et al.* [CLAS], Phys. Rev. Lett. **88**, 122001 (2002)
58. M. Ungaro *et al.* [CLAS], Phys. Rev. Lett. **97**, 112003 (2006)
59. V. V. Frolov *et al.*, Phys. Rev. Lett. **82**, 45 (1999)
60. I. G. Aznauryan *et al.* [CLAS], Phys. Rev. C **78**, 045209 (2008)
61. I. G. Aznauryan *et al.* [CLAS], Phys. Rev. C **80**, 055203 (2009)
62. H. W. Lin and S. D. Cohen, AIP Conf. Proc. **1432**, no. 1, 305 (2012) doi:10.1063/1.3701236 [arXiv:1108.2528 [hep-lat]].
63. V. D. Burkert and C. D. Roberts, Rev. Mod. Phys. **91**, no. 1, 011003 (2019) doi:10.1103/RevModPhys.91.011003 [arXiv:1710.02549 [nucl-ex]]
64. V. I. Mokeev *et al.* [CLAS], Phys. Rev. C **86**, 035203 (2012)
65. V. I. Mokeev *et al.*, Phys. Rev. C **93**, no. 2, 025206 (2016) doi:10.1103/PhysRevC.93.025206
66. G. V. Fedotov *et al.* [CLAS], Phys. Rev. C **98**, no. 2, 025203 (2018) doi:10.1103/PhysRevC.98.025203
67. E. L. Isupov *et al.* [CLAS], Phys. Rev. C **96**, no. 2, 025209 (2017) doi:10.1103/PhysRevC.96.025209
68. H. Denizli *et al.* [CLAS], Phys. Rev. C **76**, 015204 (2007)
69. C. S. Armstrong *et al.* [JLab E94014 Collaboration], Phys. Rev. D **60**, 052004 (1999)
70. H. Egiyan *et al.* [CLAS], Phys. Rev. C **73**, 025204 (2006)
71. K. Park *et al.* [CLAS], Phys. Rev. C **77**, 015208 (2008)
72. K. Park *et al.* [CLAS], Phys. Rev. C **91**, 045203 (2015)
73. I. G. Aznauryan and V. D. Burkert, Phys. Rev. C **92**, no. 3, 035211 (2015)
74. J. Segovia *et al.*, Phys. Rev. Lett. **115**, no. 17, 171801 (2015)
75. I. V. Anikin, V. M. Braun and N. Offen, Phys. Rev. D **92**, no. 1, 014018 (2015)
76. I. T. Obukhovskiy *et al.*, Phys. Rev. D **84**, 014004 (2011)
77. T. Bauer, S. Scherer and L. Tiator, Phys. Rev. C **90**, no. 1, 015201 (2014)
78. L. Tiator and M. Vanderhaeghen, Phys. Lett. B **672**, 344 (2009)
79. I. G. Aznauryan and V. Burkert, Phys. Rev. C **95**, no. 6, 065207 (2017) doi:10.1103/PhysRevC.95.065207 [arXiv:1703.01751 [nucl-th]].
80. E. Santopinto and M. M. Giannini, Phys. Rev. C **86**, 065202 (2012) doi:10.1103/PhysRevC.86.065202 [arXiv:1506.01207 [nucl-th]].
81. R. G. Moorhouse, Phys. Rev. Lett. **16**, 772 (1966). doi:10.1103/PhysRevLett.16.772
82. Z. p. Li, V. Burkert and Z. j. Li, Phys. Rev. D **46**, 70 (1992).
83. L. Lanza, talk at this workshop, A. D' Angelo *et al.*, Jefferson Lab Letter of Intent LO112-15-004 (2015).
84. L. Elouadrhiri, R. Gothe, V. Mokeev, talks at this workshop.
85. V. D. Burkert, "Jefferson Lab at 12 GeV: The Science Program," Ann. Rev. Nucl. Part. Sci. **68**, 405 (2018). doi:10.1146/annurev-nucl-101917-021129
86. V. D. Burkert, L. Elouadrhiri and F. X. Girod, Nature **557**, no. 7705, 396 (2018). doi:10.1038/s41586-018-0060-z
87. U. Özdem and K. Azizi, arXiv:1912.06375 [hep-ph].